array of $2N$ elements with optimum difference pattern performance[1] and with constant sidelobe levels. For certain sidelobe ratio/element number combinations, the Zolotarev distribution begins to increase near the array ends; the disadvantages of such a behaviour have been pointed out by Hansen.[2] Furthermore, in many practical cases a sidelobe taper is highly desirable. To solve this problem we can follow a procedure similar to that adopted by Villeneuve[3] for sum patterns, and shift the far-out Zolotarev roots so that after the first $(\bar{n}-1)$ roots they are coincident with those of a uniform sum array of $(2N+1)$ elements.

Analysis: The space factor of a Zolotarev array of $2N$ elements can be written as

$$D(s) = (s-1)\prod_{n=1}^{N-1}(s-s_n)(s-s_n^*) \quad (1)$$

where $s = e^{j\psi}$, $\psi = \beta d \sin\theta$, d is the element spacing and θ is the pattern angle measured from the broadside direction. The quantity $s_n = e^{j\psi_n}$, where the ψ_n are the Zolotarev pattern zeros (not counting the null at $\psi = 0$, which is fixed by the $(s-1)$ factor) which, as indicated above, occur in conjugate pairs.

The zeros of the sum pattern $\sin[(2N+1)\psi/2]/\sin[\psi/2]$ of a uniform array of $2N+1$ elements are given by $\psi_{0n} = n[2\pi/2N+1]$, $n = \pm1, \pm2, \ldots, \pm N$.

We now alter the Zolotarev zeros ψ_n, so that for $n \geq \bar{n}$ the nth Zolotarev zero coincides with the $(n+1)$th zero of the above uniform sum pattern. In addition to being altered, the first $(\bar{n}-1)$ zeros (excluding that at $\psi = 0$) are shifted progressively by multiplying each Zolotarev zero by a dilation factor $\sigma = (\bar{n}+1)2\pi/2N+1$.

Table 1 ARRAY PATTERN ZEROS FOR $\bar{n} = 4$

Zero index	Zolotarev array zeros (ψ_n)	Zeros (ψ_{0n}) of uniform $(2N+1)$ element sum pattern	Shifted zeros
0	0·0	±0·2991993	0·0
1	±0·6160322	±0·5983986	±0·6614926
2	±0·8172512	±0·8975979	±0·8775607
3	±1·0928009	±1·1967972	±1·1734448
4	±1·3931856	±1·4959965	±1·4959965
5	±1·7040309	±1·7951958	±1·7951958
6	±2·0200867	±2·0943951	±2·0943951
7	±2·3389902	±2·3935944	±2·3935944
8	±2·6599911	±2·6927937	±2·6927937
9	±2·9808065	±2·9919930	±2·9919930

Thus, if the new zeros are ψ_n', then for $n = 1, 2, \ldots, (N-1)$, we have

$$\psi_n' = \begin{cases} \sigma_n\psi_n & n < \bar{n} \\ (n+1)2\pi/2N+1 & n \geq \bar{n} \end{cases} \quad (2)$$

If these new roots are inserted into eqn. 1 and eqn. 1 is multiplied out into the usual polynomial form, the new element excitations can be found.

Design example: Consider a linear Zolotarev array of 20 elements (therefore a 19th-order polynomial) with a sidelobe ratio of 25 dB. The pattern zeros of such an array are given in the second column of Table 1. The zeros of the uniform sum pattern are given in the third column of Table 1. Suppose now that we choose $\bar{n} = 4$, so that $\sigma = 1{\cdot}07396$. Then the new zero positions are as given in the fourth column. From the array polynomial obtained after inserting these new zeros, we can obtain the new element excitations of the $\bar{n}$-distribution. These are given in Table 2, numbered from the centre to edge element. The corresponding array space factor is shown in Fig. 1.

Table 2 ELEMENT EXCITATIONS FOR HALF OF THE ARRAY

n	a_n	n	a_n
1	0·17775	6	0·94577
2	0·51157	7	0·82207
3	0·78170	8	0·65885
4	0·95011	9	0·46616
5	1·00000	10	0·24392

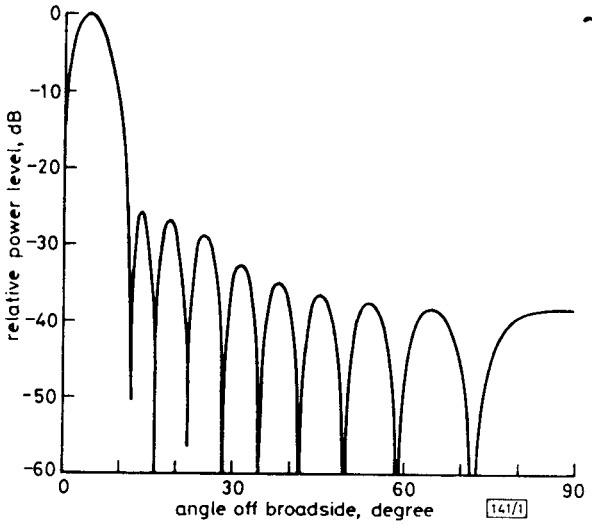

Fig. 1 *Array space factor*

Conclusion: It has been shown that a discrete, uniformly spaced array, equivalent to the Bayliss difference pattern for continuous line sources, can be developed directly. The corresponding element excitations can be found exactly, without recourse to any form of sampling of continuous distributions.

D. A. McNAMARA

Department of Electronic Engineering University of Pretoria 0002 Pretoria, S. Africa

26th November 1985

References

1 MCNAMARA, D. A.: 'Optimum monopulse linear array excitations using Zolotarev polynomials', *Electron. Lett.*, 1985, **21**, pp. 681–682

2 RUDGE, A. W., MILNE, K., OLVER, A. D., and KNIGHT, P. (Eds.): 'The handbook of antenna design' (Peter Peregrinus Ltd., London, 1984), Chap. 9

3 VILLENEUVE, A. T.: 'Taylor patterns for discrete arrays', *IEEE Trans.*, 1984, **AP-32**, pp. 1089–1093

GENERALISED COUPLED-MODE EQUATIONS AND THEIR APPLICATIONS TO FIBRE COUPLERS

Indexing terms: Optical fibres, Optical connectors and couplers

Generalised coupled-mode equations for two or more coupled weakly guiding fibres are presented, when the fibres are not well separated. These equations are applied to studying fibre couplers. Compared with the results derived from previous coupled-mode equations, our results are in better agreement with those calculated rigorously by a numerical method.

At present, fibre couplers, including multiplexers, coupler filters, polarisation splitters etc., are important optical devices in fibre optics. Usually, the coupling between modes in these devices can be described by the coupled-mode equations.[1-3] However, sometimes one cannot obtain accurate results from these equations, owing to some approximate assumptions in deriving the equations. One of these is the orthogonality relation

$$\mathrm{Re}\left[\int_{A_\infty} \boldsymbol{e}_k \times \boldsymbol{h}_i^* \cdot \boldsymbol{i}_z \, d\Omega\right] = \delta_{ki} \quad (1)$$

where A_∞ is the infinite cross-sectional area, δ_{ki} is the Kronecker delta and $\boldsymbol{i}_z$ is the unit vector in the z-direction. Eqn. 1

is not true for modes on different fibres and is a reasonable approximation when the coupled fibres are well separated. In practice, for example, in polished single-mode couplers[4,5] the coupling fibres are touching or nearly touching.

This letter presents a generalised coupled-mode equation which can be used for any separation. They are then applied to studying two coupling fibres.

First of all, we assume that the total transverse fields of the composite waveguide can be approximated by a superposition of the fields of each weakly guided fibre in isolation from the others, namely

$$\boldsymbol{E}(x, y, z) = \sum_k A_k(z)\boldsymbol{e}_k(x, y)$$
$$\boldsymbol{H}(x, y, z) = \sum_k A_k(z)\boldsymbol{h}_k(x, y) \quad (2)$$

where $\boldsymbol{e}_k$ and $\boldsymbol{h}_k$ are the transverse parts of the modal fields for the kth guided mode. There may be several modes guided on each fibre in isolation; the summations in eqn. 1 are over all the guided modes on all coupled fibres. Eqn. 2 has already been justified by Wijngaard,[6] when he studied two coupled weakly guiding optical fibres.

Based on eqn. 2, we can now proceed to formulate the generalised equations. Using eqn. 1 for modes on the same fibre and

$$g_{ki} = \mathrm{Re}\left[\int_{A_z} \boldsymbol{e}_k \times \boldsymbol{h}_i^* \boldsymbol{i}_z \, d\Omega\right] \quad (3)$$

for modes on different fibres, according to the procedure mentioned in Reference 1, we have the matrix form of the coupled-mode equations for the coupled fibres:

$$\frac{d}{dz}(\boldsymbol{GA}) + j\boldsymbol{BGA} = -j\boldsymbol{KA} \quad (4)$$

where matrix $\boldsymbol{G}$ has its diagonal elements equal to unity and offdiagonal elements equal to g_{ki}, which is zero if k and i are modes on the same fibre; $\boldsymbol{A}$ is the amplitude matrix and $\boldsymbol{K}$ is the coupling matrix with its elements

$$\kappa_{ki} = \frac{\omega\varepsilon_0}{2}\int_{A_z}(n_p^2 - n^2)\left(\boldsymbol{e}_k^* \cdot \boldsymbol{e}_i + \frac{n^2}{n_p^2}e_{zk}^* e_{zi}\right) d\Omega \quad (5)$$

where n_p denotes the composite profile and n denotes the profile of the individual fibre on which the kth mode propagates, e_{zk} and e_{zi} are the z-directed components of the modal fields, the matrix $\boldsymbol{B}$ is a diagonal matrix where its elements β_k are the propagation constants of the guided modes.

If the composite profile n_p for the coupled fibres does not change along z, eqn. 4 becomes

$$\frac{d}{dz}\boldsymbol{A} + j\boldsymbol{G}^{-1}\boldsymbol{BGA} = -j\boldsymbol{G}^{-1}\boldsymbol{KA} \quad (6)$$

Eqn. 4 or 6 is a generalised coupled-mode matrix equation, and should be more rigorous in describing the mode coupling between coupled fibres. This will be justified by studying double-core fibres.

A double-core fibre may be formed in a coupler when two fibres are close to each other. If the two cores are circular and identical as shown in the inset of Fig. 1, and if each individual one-core fibre is single-mode, then eqn. 6 is reduced to

$$\frac{d}{dz}A_k = -j(\beta + \Delta\beta)A_k - jCA_i \qquad k, i = 1, 2, i \neq k \quad (7)$$

where

$$\Delta\beta = \frac{\kappa_{kk} - g\kappa_{ki}}{1 - g^2} \quad (8)$$

$$C = \frac{\kappa_{ki} - g\kappa_{kk}}{1 - g^2}$$

where $g = g_{12} = g_{21}$, $\beta = \beta_1 = \beta_2$, $\kappa_{12} = \kappa_{21}$, $\kappa_{11} = \kappa_{22}$ due to symmetry.

When the individual one-core fibres have step-index profiles and are weakly guiding, the normalised coupling coefficients $\rho\kappa_{11}/\sqrt{(2\Delta)}$, $\rho\kappa_{12}/\sqrt{(2\Delta)}$ and g can be calculated approximately, and are plotted against the V-value in Fig. 1 in the case $d = 2\rho$, where ρ is the core radius and Δ is the relative index difference between core and cladding.

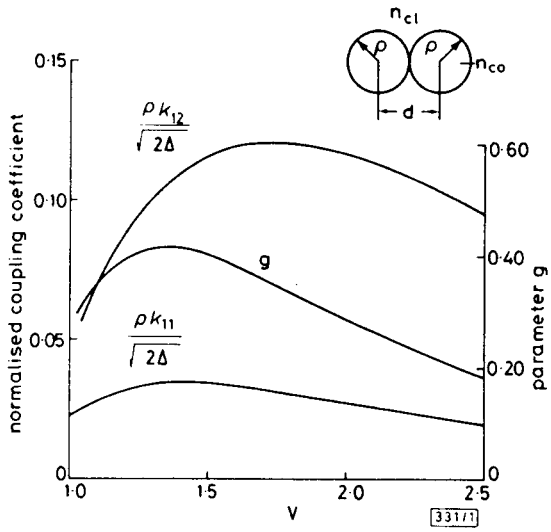

Fig. 1 *Parameter g and normalised coupling coefficients for $d = 2\rho$*

It is well known that the coupled modes can be transformed to the normal modes of the double-core fibre.[3] The propagation constants h_1 and h_2 for both normal modes are evaluated and the normalised beat length $(\rho/\sqrt{(8\Delta)})V/(h_1 - h_2)$ is shown in Fig. 2 (solid line). The broken line corresponds to $g = 0$ and the points in the Figure are cited from Wijngaard's numerical results.[6] It is obvious that our results are found to be in good agreement with his. The discrepancy between both curves is apparent when V is less than 1·7. Usually, polished couplers work at $V = 2 - 2{\cdot}4$, and, within this region, even though $g = 0{\cdot}2 - 0{\cdot}25$, the nonorthogonality between modes can still be ignored. However, for couplers working in a wide wavelength band, such as filters or wavelength-division multiplexers, it is necessary to take the nonorthogonality into account.

The curves in Fig. 2 stop at the cutoff V-value for the second mode, which can easily be calculated by setting the propagation constant of the second-order mode equal to kn_{cl}. Its solution $V_c = 1{\cdot}38$. This is exactly the same as the recent result given by Love *et al.*[7]

In conclusion, the coupled-mode equations for coupled fibres are generalised for any separation between fibres. Using them, we can obtain satisfactory results for double-core fibre. Compared with the results derived from the previous coupled-mode equations, it seems that the previous equations are valid in describing power transfer even in touching fibres provided that $V > 1{\cdot}7$.

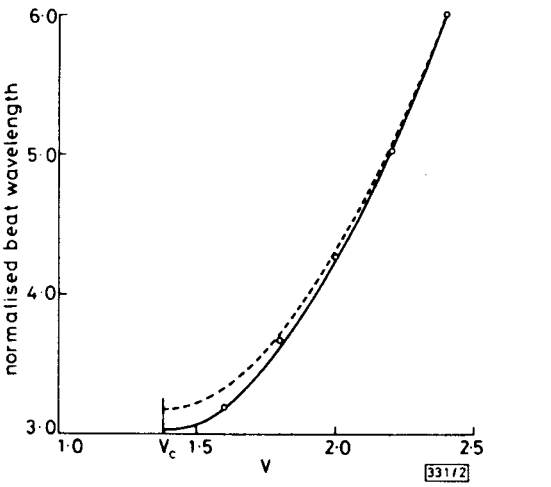

Fig. 2 *Normalised beat length calculated by generalised equations (solid line) and by previous equations (broken line)*

Acknowledgments: The author wishes to express thanks to Prof. W. A. Gambling for providing a stimulating research atmosphere, and would like to acknowledge Dr. D. N. Payne and Dr. C. D. Hussey for helpful suggestions. Financial support from the British Council is also gratefully acknowledged.

JING-REN QIAN* *20th January 1986*

Department of Electronics & Information Engineering
The University
Southampton SO9 5NH, United Kingdom

* On leave from University of Science & Technology of China, Hefei, Anhui, People's Republic of China

References

1 SNYDER, A. W.: 'Coupled-mode theory for optical fibres', *J. Opt. Soc. Am.*, 1972, **62**, pp. 1267–1277
2 MCINTYRE, P., and SNYDER, A. W.: 'Power transfer between optical fibres', *ibid.*, 1973, **63**, pp. 1518–1527
3 SNYDER, A. W., and LOVE, J. D.: 'Optical waveguide theory' (Chapman & Hall, London, 1983), Chaps. 18 and 29
4 WHALEN, M. S., and WALKER, K. L.: 'In-line optical-fibre filter for wavelength multiplexing', *Electron. Lett.*, 1985, **21**, pp. 724–725
5 MARCUSE, D.: 'Directional-coupler filter using dissimilar optical fibres', *ibid.*, 1985, **21**, pp. 726–727
6 WIJNGAARD, W.: 'Guided normal modes of two parallel circular dielectric rods', *J. Opt. Soc. Am.*, 1973, **63**, pp. 944–954
7 LOVE, J. D., and ANKIEWICZ, A.: 'Modal cut-offs in single- and few-mode fibre couplers', *IEEE J. Lightwave Technol.*, 1985, **LT-3**, pp. 100–110

EFFECT OF VARACTOR *Q*-FACTOR ON TUNING SENSITIVITY OF MICROWAVE OSCILLATORS, INCLUDING REVERSE TUNING

Indexing terms: Microwave devices and components, Microwave oscillators, Varactors

It is shown how the effect of resistive losses in a varactor diode can drastically affect the tuning characteristics of millimetre-wave oscillators and can even cause the oscillator to tune in the reverse direction.

Varactor diodes are the only tuning devices which can be used for fast tuning and high-frequency modulation (FM) of microwave solid-state oscillators. At millimetre-wave frequencies the parasitic effect of device packages plays a large part in determining the frequency of operation and the electronic tuning range of a varactor-tuned oscillator. The solid-state power device and varactor diode are generally mounted in a microwave cavity, and the resulting oscillator circuit consists of a complex circuit containing lumped and distributed elements. Aitchison[1,2] showed that, by a suitable choice of packaged devices and microwave cavity dimensions, the electronic tuning range could be very large. He argued that if a distributed element represented an inductance, then the inductive reactance is $WL(w)$, and he showed that as w changes $L(w)$ could result in an enhanced tuning range.

However, he ignored the effects of varactor loss resistance. The varactor loss only becomes significant at the higher microwave frequencies where the varactor Q-factors are very low. The varactor Q-factor is inversely proportional to frequency, and at the higher microwave frequencies high Q-factor GaAs varactors are used in preference to silicon varactors.

A varactor-tuned millimetre-wave waveguide-mounted Gunn oscillator is shown in Fig. 1. The Gunn diode is a Plessey integral heat sink device type TEO 151 and the varactor diode is a Plessey GaAs Schottky barrier diode type GAV10. The distance between the Gunn and varactor diodes and the distance from the varactor to the short-circuit can be changed by inserting suitable spacers as shown in Fig. 1. Increasing either of these distances results in a reduction in the centre frequency, and decreasing either of these distances results in an increase in frequency. By increasing one distance and decreasing the other, the centre frequency can be kept the same, but the way in which the varactor diode is coupled to the Gunn diode and cavity is entirely different. This results in a modification of the frequency/varactor voltage or tuning characteristic.

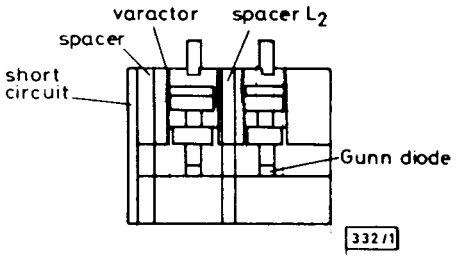

Fig. 1 *Varactor-tuned oscillator*

The tuning characteristics for four combinations of Gunn to varactor and varactor to short-circuit spacing are shown in Fig. 2. It is evident from Fig. 2 that the shape of the tuning characteristic is very dependent on how the Gunn device and varactor are coupled and, as is shown in Fig. 3, on the series resistance or Q-factor of the varactor diode. The spacers were adjusted to keep the centre frequency constant, and it is evident that by suitable choice of coupling the shape of the oscillator tuning characteristic changes completely and the oscillator can be made to tune backwards for part or even the whole of its tuning characteristic.

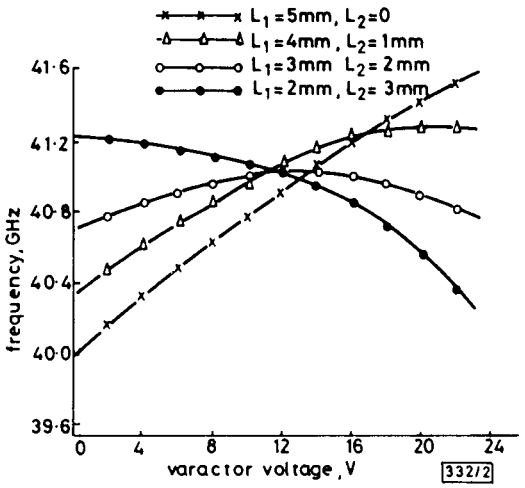

Fig. 2 *Oscillator tuning characteristics*

To investigate the effect of varactor Q-factor on the tuning characteristics of this oscillator, the circuit was modelled using the microwave circuit analysis program Touchstone. This enabled the electronic tuning characteristic to be observed as a function of varactor Q-factor and the results are shown in Fig. 3. It is evident that the shape of the tuning characteristics

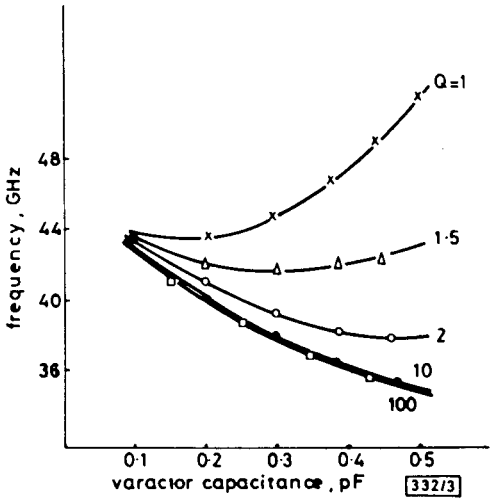

Fig. 3 *Dependence of tuning characteristic on varactor Q-factor*